



Semnan University

Mechanics of Advanced Composite Structures

Journal homepage: <https://macs.semnan.ac.ir/>ISSN: [2423-7043](#)

Research Article

Improving Prediction of Compressive Strength of Rectangular/Square (R/S) FRP-Confined Concrete Using Machine Learning

Mohammad Ghasemi ^{a*}, Yaser Moodi ^b, Seyed Rohollah Mousavi ^c

^a Assistant Professor, Department of Civil Engineering, Velayat University, Iranshahr, Iran.

^b Assistant Professor, Civil Engineering Department, Sirjan University of Technology, Sirjan, Iran.

^c Associate Professor, Civil Engineering Department, University of Sistan and Baluchestan, Zahedan, Iran

ARTICLE INFO

ABSTRACT

Article history:

Received:

Revised:

Accepted:

Keywords:

Extreme Learning Machine;
Adaptive Neural Fuzzy Inference
System;
Marine Predators Algorithm;
Kriging;
Compressive strength;

Several experimental studies have been conducted on concrete confined with FRP sheets, and various models have been proposed in previous research to determine its compressive strength. However, studies have shown that Machine Learning (ML)-based methods offer higher accuracy than these models. In this study, the effectiveness of different machine learning methods is investigated for predicting the ultimate compressive strength of Rectangular/Square (R/S) FRP-confined concrete columns. These methods include ELM, GMDH, ANFIS, and the Kriging interpolation method. Also, this study proposes utilizing optimization science as a solution to enhance the performance of the ANFIS method. As an innovation in this study, the Marine Predators Algorithm (MPA), a nature-inspired metaheuristic, has been used to optimize the parameters of the ANFIS method. To show the ability of ML methods to estimate compressive strength, statistical indices were calculated and ML methods were compared; the correlation coefficient (R^2) for ELM, GMDH, ANFIS, ANFIS-MPA, and Kriging interpolation methods was equal to 0.89, 0.92, 0.92, 0.93, and 0.98, respectively. Also, these results show that the proposed methods have better performance than the best models in previous studies, with an average error reduction of 62%.

© 2025 The Author(s). Mechanics of Advanced Composite Structures, published by Semnan University Press.

This is an open access article under the CC-BY 4.0 license. (<https://creativecommons.org/licenses/by/4.0/>)

1. Introduction

In civil engineering, FRP is widely used due to its high strength-to-weight ratio. One of the applications of FRP is the confinement of concrete with FRP sheets to increase its compressive strength. Due to the lateral expansion of concrete, FRP confinement in the hoop direction has received significant attention. The effect of various parameters, such as the shape and dimensions of the cross-section, the compressive strength of concrete, and the type of FRP, has been experimentally investigated in previous studies. The first experimental study on FRP-confined concrete was presented by Nanni

and Bradford [1]. Three kinds of FRP were used for confining concrete with ordinary strength under uniaxial compressive loading. The results of their study showed that compressive strength and ductility increase with FRP confinement. Early research attempted to develop analytical models for FRP-confined concrete based on those previously used for steel plates [2, 3]. Later researchers realized that the results of these models were incorrect and non-conservative [4]. After that, different models were presented to determine the compressive strength of concrete confined with FRP [5–21]. It is noteworthy that the majority of these models are empirical and

* Corresponding author.

E-mail address: m.ghasemi@velayat.ac.ir

Cite this article as:

Mohammadi, A. and Mahdi-Nia, M., 2025. Title of article. *Mechanics of Advanced Composite Structures*, 12(1), pp. xx-xx

<https://doi.org/10.22075/MACS.2024.39315.2050>

calibrated based on a limited number of experimental data.

Recently, artificial intelligence methods have been widely used in various fields of civil engineering due to their ability to simulate complex processes. [22–28]. Ilkhani et al. [29] proposed a shear strength estimation relationship for reinforced concrete beam-column joints strengthened by FRP using neural networks. In 2019, Rezaie-Balf [30], gathered data from 228 experimental case studies focused on scour depth downstream of sluice gates with an apron. Using multivariate adaptive regression splines (MARS), they derived a predictive relationship for scour depth through detailed data analysis. Saha et al. [31] used gradient boosting, Adaboost, LightGBM, XGBoost, and CatBoost to predict the fresh and hardened properties of self-compacting concrete. Gradient Boosting Regressor, Extra Tree Regressor, Deep Neural Network, and One-Dimensional CNN were used for predicting the self-consolidating concrete blends composed of recycled plastic aggregates by Ali et al. [32]. A predictive model for impact-loaded composite panels was developed using artificial neural networks (ANN) and adaptive network-based fuzzy inference systems (ANFIS), demonstrating their effectiveness in estimating structural response under dynamic conditions [33]. Machine learning methods include Bayesian posterior models, back-propagation artificial neural networks, multi-gene genetic programming, and support vector machine models used for estimating the ultimate axial strain of confined concrete by Chen et al. [34]. Moodi et al. [35] used the RSM method for estimating the relative bond strength of corroded bars in lap-spliced RC beams. In 2019, DeRousseau [36] compared various ML methods such as linear regression, polynomial regression, kernelized support vector regression, kernelized Gaussian process, regression trees, boosted trees, and random forest to predict the compressive strength of field-placed concrete. In the Naderpour et al. [37] study, the flexural strength of ferrocement members was evaluated by GMDH. In 2020, Kummar et al. [38] developed an ANFIS model for the prediction of the surface roughness of the thermally drilled hole. In Amirkhani [39] DNA-binding remains in local parts of protein sequences were predicted by the Fuzzy Cognitive Map (FCM) model.

Cihan [40] showed that the fuzzy logic method provides more accurate predictions than any other regression method for estimating concrete compressive strength and slump. In predicting the bond strength between concrete and FRP sheets, Gaussian Process Regression (GPR) was compared with Regression Tree, ANN, SVM, and

Multiple Linear Regression (MLR). The results showed that GPR achieved the highest accuracy.

In 2020, Faramarzi et al. [41] proposed MPA, a swarm intelligence algorithm inspired by the Lévy and Brownian search strategies used by ocean predators to locate prey. The Lévy approach is utilized in prey-rich environments, while the Brownian method is preferred in prey-scarce conditions. MPA has demonstrated effectiveness in solving a wide range of problems in diverse research fields.

In previous research, researchers have employed various machine-learning methods to estimate the compressive strength of columns confined by FRP sheets, both for circular and square/rectangular cross-sections. Table 1 provides a summary of these studies, including the number of specimens used, the machine learning method applied, and the type of cross-section (circular and R/S). It is evident from Table 1 that there have been relatively fewer studies that specifically focused on using machine learning methods for estimating the compressive strength of R/S concrete confined by FRP. This suggests that there might be a potential area for further exploration and research in this specific domain.

In this study, the researchers collected experimental data from rectangular/square (R/S) concrete specimens confined by FRP from previous studies. To ensure a more reliable modeling process, a wider range of statistical populations was considered compared to previous research efforts, resulting in a comprehensive database comprising 485 specimens.

A key contribution of this study is the application of ELM, GMDH, ANFIS, and Kriging interpolation methods for predicting the compressive strength of R/S FRP-confined concrete, which, to the best of our knowledge, has not been explored in previous studies. Additionally, while meta-heuristic algorithms have been extensively employed for parameter optimization in various engineering and computational fields, this study is the first to utilize the Marine Predators Algorithm (MPA) to optimize the parameters of the ANFIS model. This novel ANFIS-MPA approach, along with other ML models, is used for the first time to estimate the compressive strength of R/S concrete confined by various FRP types. The results indicate that Kriging interpolation achieves the highest accuracy, with a correlation coefficient of 0.98, outperforming other methods. Furthermore, replacing the Mamdani system with MPA in the ANFIS method reduces the total error by 12% across all specimens, demonstrating the effectiveness of this optimization strategy.

Table 1. Approaches for predicting the compressive strength of FRP-confined columns

Study	Year	Section(s)	Method(s)	Types of concrete	Number of specimens
Jin et al. [42]	2010	Rectangular, Circular	RBFNN	Plain	154, 362
Pham and Hadi [43]	2014	Rectangular	ANN	Plain	209
Doran et al. [44]	2015	Rectangular	MFIS	Plain	140
Lim et al. [45]	2016	Circular	GP	Plain	832
Moodi et al. [11]	2018	Rectangular	RSM	Plain	416
Sharifi et al. [46]	2019	Rectangular	ANN	Plain	190
Mohana [47]	2019	Rectangular	ANN, SVR	RC	163
Moodi et al. [48]	2021	Rectangular	ANN, SVR	Plain	463

2. Some Existing Models of Previous Studies

In previous studies, different methods have been proposed to estimate the compressive strength of R/S FRP-confined concrete. To compare the methods of this study with previous studies, some of which are summarized in Table 2 of Moodi et al. [48] study was used.

3. Experimental Data

Many tests have been done on concrete confined by FRP. Among these tests, the share of circular specimens is higher than rectangular specimens. However, due to stress concentration in rectangular specimens, these specimens have more complexity than circular specimens. Therefore, providing a model using a comprehensive database can be of great help in providing a community model to estimate the compressive strength of these specimens. In this study, a comprehensive statistical population including 485 S/R specimens confined by FRP types, extracted from various types of research, was used. In this statistical comprehensive, it has been made to collect all kinds of specimens available in past studies. Therefore, the range of variable changes is large. In this statistical population, there are concretes with different types of strength (normal-strength concrete and high-strength concrete). The types of FRP used in this data—CFRP, AFRP, and GFRP—are summarized under the headings C, A, and G in Table 2, respectively. All the FRP wraps used in this data are unidirectional or unidirectional (with ring direction). The details of the specimens are given in Table 2. In this table, b and h , the length and width of the specimens (cm), f_c is the compressive strength of unconfined concrete (MPa), and r is the corner radius of the concrete section (cm).

It is worth mentioning that in this dataset, 44 concrete specimens had a confined compressive strength lower than that of unconfined concrete. Therefore, these specimens were identified as outliers and removed from the dataset. Information on the outlier data is not included in

Table 2. Seventy percent (309 samples) of the data were used for training, while the remaining 132 samples were used for testing.

By correctly knowing the data and knowing their statistical details, a better understanding of them can be obtained. For this purpose, the histogram diagram to show the distribution of each of the mentioned parameters can be seen in Fig. 1. Also, the normal fitting diagram of the data is drawn on the histogram of the data. Fig. 2 shows the correlation matrix of the considered data for determining compressive strength. The variables included are b , h , r , f_{co} , t_f , F_f , E_f , and F_{cc} . The heatmap highlights the degree of linear relationship between these variables, with values close to 1 or -1 indicating strong positive or negative correlations, respectively. Also, the range of variables of this database is presented in Table 3.

4. Extreme Learning Machine (ELM)

Huang et al. [87] introduced the Extreme Learning Machine, which has gained significant attention due to its remarkably fast training process and strong generalization capabilities. ELM is a modern algorithm designed for single-hidden-layer feedforward neural networks, with applications in statistical classification, regression tasks, and clustering. ELM is based on the empirical theory that minimizes risk and avoids multiple repetitions and local minimization because the learning process requires only one repetition [88]. Due to better generalizability, controllability, and fast learning speed, it has been used in various fields and applications.

The ELM model employs a straightforward three-step construction process [89]: (i) weights and biases are randomly initialized, avoiding the iterative approach typical of ANN methods; (ii) the input data is processed through hidden layer parameters to generate the hidden layer output matrix; and (iii) the Moore-Penrose generalized inverse is applied to the hidden layer output matrix, allowing for the inversion needed to calculate output weights and solve a system of linear equations.

Table 2. Details of the database

Reference	n	n'	Type of FRP	$b(cm)$	$h(cm)$	$r(cm)$	f'_c
[49]	8	8	C	15	15	0.5-5	26.7-31.8
[50]	6	6	G	10	10	0-1.6	54.8
[51]	2	2	C	15	15	0.3	13
[52]	1	1	C	15.2	15.2	0.3	20.1
[53]	4	4	C	15	15	1-3	33.5-36.5
[54]	24	24	C	9.525-13.335	13.335-19.05	2.54	21.4-55.4
[55]	5	4	C, G	15.2	15.2	0.5	32.3-42.2
[56]	1	1	C	15	15	2.5	10
[5]	9	9	C	7.9-13.2	13.2-21.4	1.5	18.9-21.5
[57]	4	4	G	15.2	15.2	1.1-2.5	31.2-32.4
[58]	1	1	C	20	20	3	38.1
[59]	3	3	C	10-10.5	10-20	1	32.3
[6]	12	10	C	15-25	25-30	4	32.8-34
[7]	12	12	C	15	15-22.5	1.5-2.5	24-41.5
[60]	15	15	C	10-15	10-15	2.5	21.3-25.7
[61]	9	8	C	15.25	15.25	0.635	40.6
[62]	6	6	C, G	15	15-20	1-2.5	17.6-25
[63]	2	2	C	10.8	10.8	0.826	22.6
[64]	26	24	C, A	15.2	15.2-20.3	0.5-3.8	35.8-43.9
[65]	15	15	C, G	20	20	3	33-39.9
[66]	4	4	C, G	20	20	3	25.5
[67]	8	8	C	9.4-15	15-18.8	1	23.7-29.5
[68]	14	13	C, G, A	15	15	0.5-2.5	33.9-36.7
[69]	24	24	C	15	15-30	2-5	19.5-49.5
[70]	60	59	C	15	15	0-6	29.3-55.2
[71]	9	9	A	10	10	1	46.4-101.2
[72]	15	15	A	7-15	7-15	0.7-1.5	34.6-52.1
[73]	10	10	C	10-40	10-40	1-4.5	24.4
[74]	8	8	C	20.4-30.5	20.4-30.5	2-3	25.5
[75]	30	22	C	15	15-30	3	32.3-42.4
[76]	2	2	C, G	27.9	27.9	1.9	15.2
[77]	28	26	C	15-45	15-60	3	20.6
[78]	37	31	C, G	25.4-38.1	38.1	3.8	29.2-38.7
[79]	2	2	A	15	15	1.5	45-50
[80]	15	6	C	15-20	20-30	1-4	24-26.7
[81]	24	11	C	11.25-15	15-22.5	1.5-3	107.3-110.8
[82]	24	19	C	11.25-15	15-22.5	1.5-3	76.6-79.6
[83]	4	4	A	15	15	3	98.2
[84]	2	2	C	15	15	3	104.8
[85]	4	3	C	15	15-22.5	2.5	93.8-106
[86]	4	4	C	11.25-15	15-22.5	1.5-3	107.8

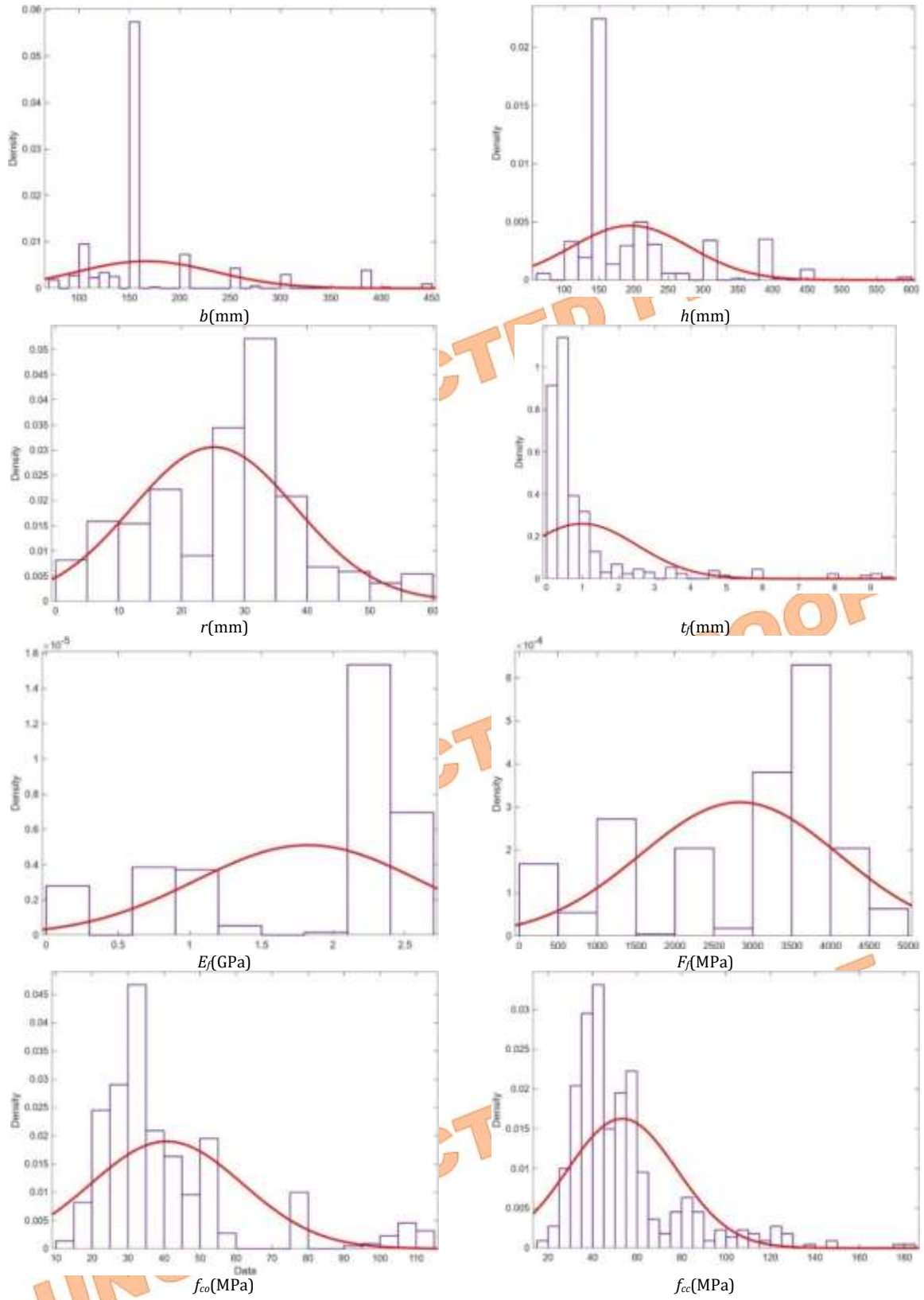


Fig. 1. Histogram diagram of the data

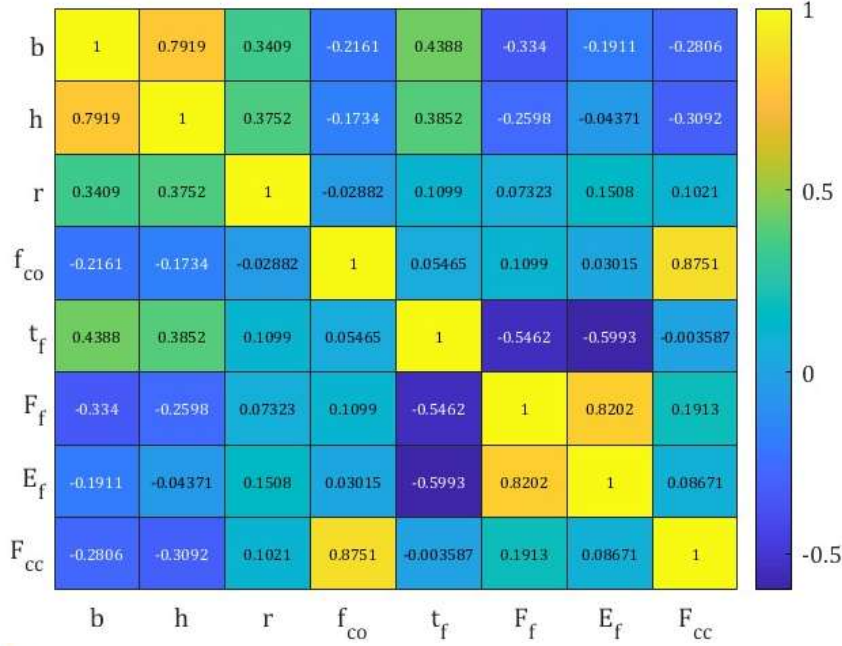


Fig. 2. Correlation matrix of variables affecting confined-FRP compressive strength

Table 3. The range of variables

Variable	Range
Width (b)	70-450 mm
Length (h)	70-600 mm
Corner radius (r)	0-60 mm
Compressive strength (f _{co})	10-110.8 MPa
Different types of FRPs	CFRP, AFRP, and GFRP
Modulus of elasticity of FRP (E _f)	10.3—257 GPa
FRP thickness (t _f)	0.072-9.6 mm
Tensile strength of FRP (F _f)	154—4830 GPa

For a set of training examples (N number), (x_i, t_i) , where $(x_i, t_i) \in R^{n \times R^m}$ ($i=1,2,\dots, N$), the output of a single hidden layer feedforward neural networks (SLFN) with L hidden neurons and an activation function $f(x)$ can be represented as follows [87]:

$$\sum_{i=1}^L \beta_i f_i(x_j) = \sum_{i=1}^L \beta_i f(a_i \cdot x_j + b_i) = t_j, \quad (1)$$

$j = 1, \dots, N$

where $a_i = [a_{i1}, a_{i2}, \dots, a_{in}]^T$ is the vector of weights that connect the i th hidden neuron to the input neurons, b_i is the bias weight of the i th hidden neuron, $\beta_i = [\beta_{i1}, \beta_{i2}, \dots, \beta_{im}]$ is a weight vector that connects i th hidden node to the output nodes, $a_i \cdot x_j$ is the inner product of a_i and x_j . The activator function can be selected from one of the "Sigmoid", "Sine", and "RBF" functions. Then, Eq. (1) can be written as follows. [87]:

$$H\beta = T \quad (2)$$

where:

$$H(a_1, \dots, a_L, b_1, \dots, b_L, x_1, \dots, x_N) = \begin{bmatrix} f(a_1 \cdot x_1 + b_1) & \dots & f(a_L \cdot x_1 + b_L) \\ \vdots & & \vdots \\ f(a_1 \cdot x_N + b_1) & \dots & f(a_L \cdot x_N + b_L) \end{bmatrix}_{N \times L} \quad (3)$$

$$\beta = \begin{bmatrix} \beta_1^T \\ \vdots \\ \beta_L^T \end{bmatrix}_{L \times m} = \begin{bmatrix} \beta_{11} & \dots & \beta_{1m} \\ \vdots & \ddots & \vdots \\ \beta_{L1} & \dots & \beta_{Lm} \end{bmatrix} \quad (4)$$

$$\beta = \begin{bmatrix} t_1^T \\ \vdots \\ t_L^T \end{bmatrix}_{L \times m} = \begin{bmatrix} t_{11} & \dots & t_{1m} \\ \vdots & \ddots & \vdots \\ t_{L1} & \dots & t_{Lm} \end{bmatrix} \quad (5)$$

where H is the hidden layer output matrix of ELM, T is the training data target matrix, and the i th column of H is the i th hidden node output to inputs x_1, x_2, \dots, x_N .

The output weights β can be calculated using the following equation:

$$\beta = H^+ T \quad (6)$$

where H^+ is the Moore-Penrose generalized inverse of H [90].

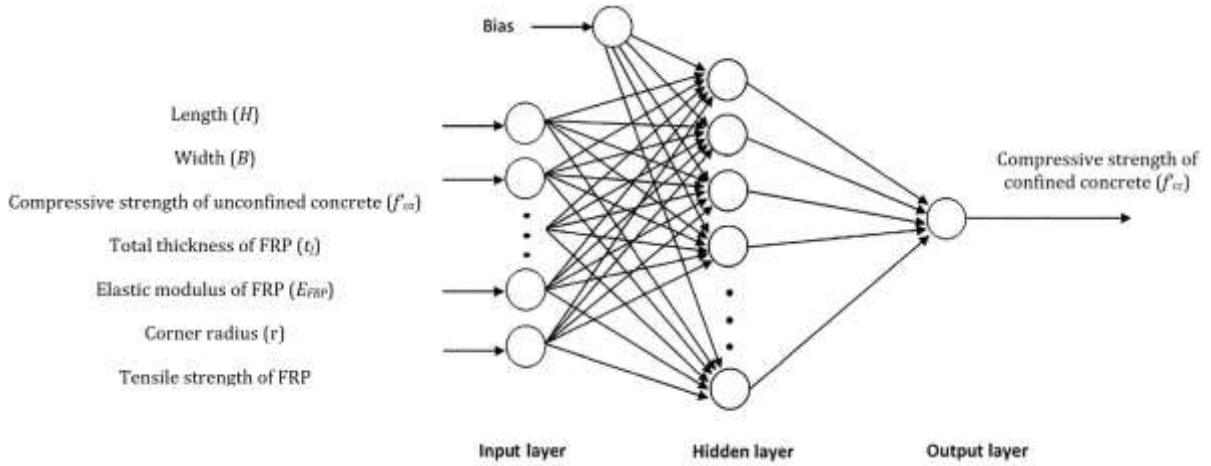


Fig. 3. Architecture of the ELM model used to predict the compressive strength of confined concrete.

5. Group Method of Data Handling (GMDH)

The Group Method of Data Handling (GMDH) is a prediction model presented by Ivakhnenko [91]. It employs regression-based algorithms, heuristic self-organizing principles, and automatic model optimization. GMDH is mainly used for multivariate analysis to model complex functions with multiple variables. In the GMDH neural network, input variables are linked to output variables through a nonlinear function known as the Kolmogorov-Gabor polynomial [92, 93]. This polynomial function is used to describe the relationships between the input and output variables in the model:

$$y = a_0 + \sum_{i=1}^m a_i x_i + \sum_{i=1}^m \sum_{j=1}^m a_{ij} x_i x_j + \sum_{k=1}^m \sum_{j=1}^m \sum_{i=1}^m a_{ijk} x_i x_j x_k + \dots \quad (7)$$

where m is the number of input variables, x is the input variable, y is the model output, and a is the coefficients in the Kolmogorov-Gabor polynomial that is solved by the regression method. Considering this, a quadratic polynomial applied in the GMDH network can be written as:

$$G(x_1, x_2) = \hat{y} = a_0 + a_1 x_1 + a_2 x_2 + a_{11} x_1^2 + a_{22} x_2^2 + a_{12} x_1 x_2 \quad (8)$$

The objective function of the GMDH-NN is to minimize the squared error between the predicted outputs and the actual outputs. Mathematically, the objective function can be represented as:

$$\sum_{i=1}^m [(\hat{y}_i - y_i)]^2 \rightarrow \min \quad (9)$$

The weighting coefficients of a quadratic function (G_i) are obtained through optimization to achieve the best fit between the input-output datasets used for training. Mathematically, G_i can be written as [25]:

$$E = \frac{\sum_{i=1}^m [(G_i(x_i, x_j) - y_i)]^2}{m} \quad (10)$$

By placing Eq. 10 in partial derivative, a matrix equation ($Aa = Y$) is obtained, wherein [94]:

$$a = \{a_0, a_1, a_2, a_{11}, a_{22}, a_{12}\} \quad (11)$$

$$Y = \{y_1, \dots, y_m\}^T \quad (12)$$

$$A = \begin{bmatrix} 1 & x_{1p} & x_{1q} & x_{1p}x_{1q} & x_{1p}^2 & x_{1q}^2 \\ 1 & x_{2p} & x_{2q} & x_{2p}x_{2q} & x_{2p}^2 & x_{2q}^2 \\ \dots & \dots & \dots & \dots & \dots & \dots \\ 1 & x_{mp} & x_{mq} & x_{mp}x_{mq} & x_{mp}^2 & x_{mq}^2 \end{bmatrix} \quad (13)$$

The Matrix equation ($Aa = Y$) is solved by using the singular value decomposition method. In this method, a is calculated based on [95]:

$$a = (A^T A)^{-1} A^T Y \quad (14)$$

In this study, an advanced version of the GMDH neural network was utilized, where more than two variables are initially selected, enabling the formation of higher-order polynomial relationships.

6. Fuzzy System Theory (FIS)

The theory of fuzzy sets was first proposed by Zadeh [96]. Over time, this theory has been well-received in various fields, so now fuzzy sets are used in all fields of industry and various sciences. Applications of fuzzy inference systems include designing a decision support system, dynamic system identification, interpolation, approximation, estimation, and so on. Indeed, one of the most significant advantages of fuzzy logic is its capability to handle and represent uncertainty in a parametric or structural context. Additionally, it serves as a novel tool for addressing problems where probability theory lacks applicability. The fuzzy inference system establishes a nonlinear mapping between input and output, effectively processing the input using a set of rules and converting it to the output. These rules are obtained through human knowledge, consciously and empirically, or unconsciously and empirically. A membership function can be defined for each input or output in a fuzzy logic system. These functions are

responsible for mapping the membership value, which lies between 0 and 1, of each point in the input or output space [97]. Trimf, Trapmf, Dsigmf, Gussmf, etc., are among the membership functions in fuzzy systems [98]. Fig. 4 illustrates the steps of a fuzzy system along with the membership functions employed in this research.

The Mamdani fuzzy system and the Takagi-Sugeno-Kang fuzzy system (TSK), better known as Sugeno, are among the most widely used fuzzy inference systems. The fuzzy system utilized in this research is the Mamdani system. This system is particularly well-suited for decision support systems due to its intuitive and interpretive nature of the rules. It allows for a clear representation and understanding of the fuzzy rules and their implications. Moreover, the Mamdani system can be implemented in different configurations, including multi-input and multi-output, as well as multi-input and single-output setups, providing flexibility in modeling complex

relationships and decision-making processes. The Mamdani inference system employs fuzzy sets as outputs for its rules, producing results that are both nonlinear and fuzzy [99].

7. ANFIS

In 1993, Jang introduced the fuzzy neural model, which was a pioneering approach that combined the principles of artificial neural networks and fuzzy systems. [100]. The most important feature of this system is the simultaneous use of neural network learning capabilities and the transfer of human knowledge using fuzzy logic to the desired system. ANFIS is trained using an input and output database and then creates a fuzzy system (FIS) that allows for the prediction and estimation of various phenomena in different scientific fields. Fig. 5 illustrates the flowchart of a fuzzy neural system. [101].

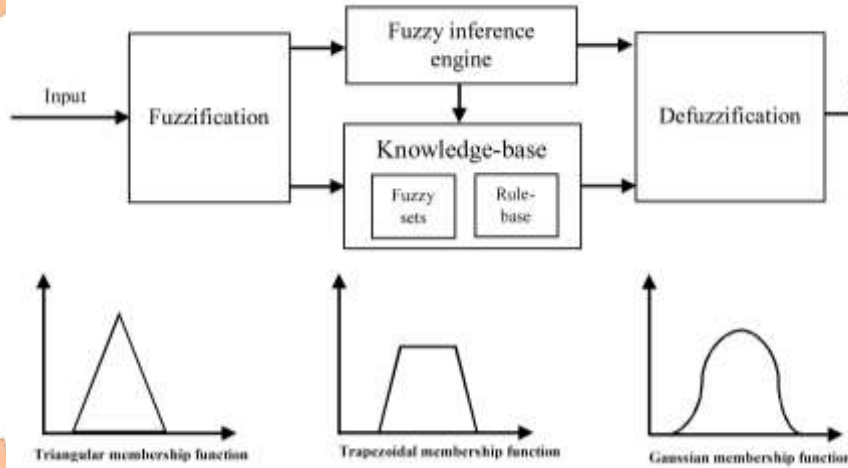


Fig. 4. Fuzzy System Structure [102]

8. Combining Fuzzy System with MPA (ANFIS-MPA)

The optimization method, developed by Faramarzi et al. [41], is inspired by nature and based on various foraging strategies (Lévy and Brownian) observed in marine predators. The MPA optimization process simulates predator-prey interactions and is divided into three main stages: (1) the prey moves faster than the predator, (2) both the predator and prey move at the same speed, and (3) the predator moves faster than the prey. In each stage, the predator's optimal movement is used to determine the step size towards the prey. During the first stage, the predator remains stationary; in the second, it follows Brownian motion; and in the third, it adopts the Lévy strategy. Each stage corresponds to one-third of the total iterations.

The mathematical modeling of these three phases is given in Eqs. 15 to 18.

The 1st. phase: ($V_{\text{predator}} < V_{\text{prey}}$)

$$\begin{aligned} \overrightarrow{\text{stepsize}}_i &= \vec{R}_B \otimes (\overrightarrow{\text{Elite}}_i - \vec{R}_B \otimes \overrightarrow{\text{Prey}}_i) \\ i &= 1, \dots, n \\ \overrightarrow{\text{Prey}}_i &= \overrightarrow{\text{Prey}}_i + P \cdot \vec{R} \otimes \overrightarrow{\text{stepsize}}_i \end{aligned} \quad (15)$$

where \vec{R}_B = random-numbers vector (based on Normal distribution); \otimes = entry-wise multiplications; $P = 0.5$; \vec{R} = a random numbers vector in $[0,1]$.

The 2nd. phase: ($V_{\text{predator}} = V_{\text{prey}}$)

For the primary half of the populace

$$\begin{aligned} \overrightarrow{\text{stepsize}}_i &= \vec{R}_L \otimes (\overrightarrow{\text{Elite}}_i - \vec{R}_L \otimes \overrightarrow{\text{Prey}}_i) \\ i &= 1, \dots, n/2 \\ \overrightarrow{\text{Prey}}_i &= \overrightarrow{\text{Prey}}_i + P \cdot \vec{R} \otimes \overrightarrow{\text{stepsize}}_i \end{aligned} \quad (16)$$

where \vec{R}_L = random-numbers vector (based on Lévy distribution); For the second half of the populace

$$\begin{aligned} \overrightarrow{\text{stepsize}}_i &= \vec{R}_B \otimes (\vec{R}_B \otimes \overrightarrow{\text{Prey}}_i) \\ i &= n/2 + 1, \dots, n \\ \overrightarrow{\text{Prey}}_i &= \overrightarrow{\text{Elite}}_i + P \cdot CF \otimes \overrightarrow{\text{stepsize}}_i \end{aligned} \quad (17)$$

where $CF = \left(1 - \frac{\text{Iter}}{\text{MaxIt}}\right)^{\left(\frac{\text{Iter}}{2 \cdot \text{MaxIt}}\right)}$

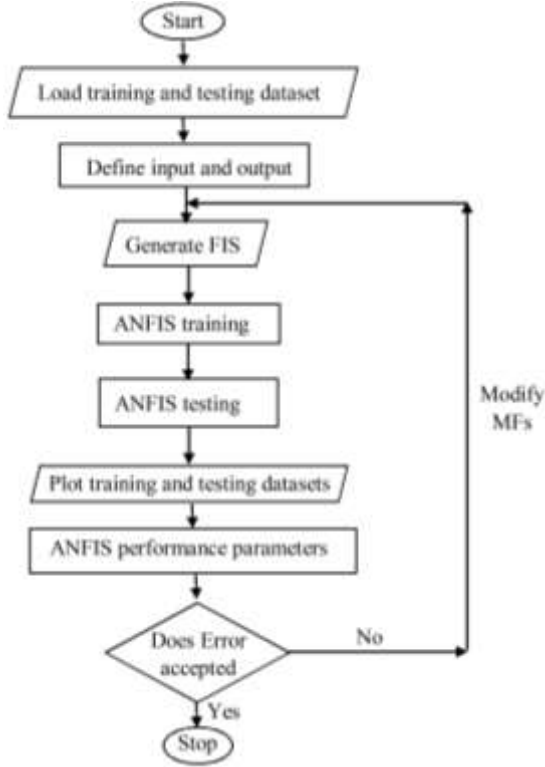


Fig. 5. Flowchart of the ANFIS process [103]

The 3rd. phase: ($V_{\text{predator}} > V_{\text{prey}}$)

$$\begin{aligned} \text{stepsize}_i &= \bar{R}_L \otimes (\bar{R}_L \otimes \text{Elite}_i - \text{Prey}_i) \\ i &= 1, \dots, n \\ \text{Prey}_i &= \text{Elite}_i + P.CF \otimes \text{stepsize}_i \end{aligned} \quad (18)$$

Impact of FADs: Fish Aggregating Devices (FADs) are environmental concerns that affect the behavior of marine predators [104]. Incorporating FADs into the algorithm helps prevent the algorithm from getting stuck in local optima. The mathematical modeling of this effect is represented by Equation 19:

$$\begin{aligned} \text{Prey}_i &= \text{Prey}_i + CF[\bar{X}_{\min} + \bar{R} \otimes (\bar{X}_{\max} - \bar{X}_{\min})] \otimes \bar{U} \\ \text{Prey}_i &= \text{Prey}_i + [\text{FADs}(1 - r) + r](\text{Prey}_{r1} - \text{Prey}_{r2}) \end{aligned} \quad \text{if } R \leq \text{FADs} \quad (19)$$

where $\text{FADs} = 0.2$; \bar{U} = a binary vector (It is a random vector, values greater than 0.2 become one, and values less than 0.2 become zero.); r = a random number between 0 and 1.

The overall process of the marine predator's algorithm is given in Fig. 6.

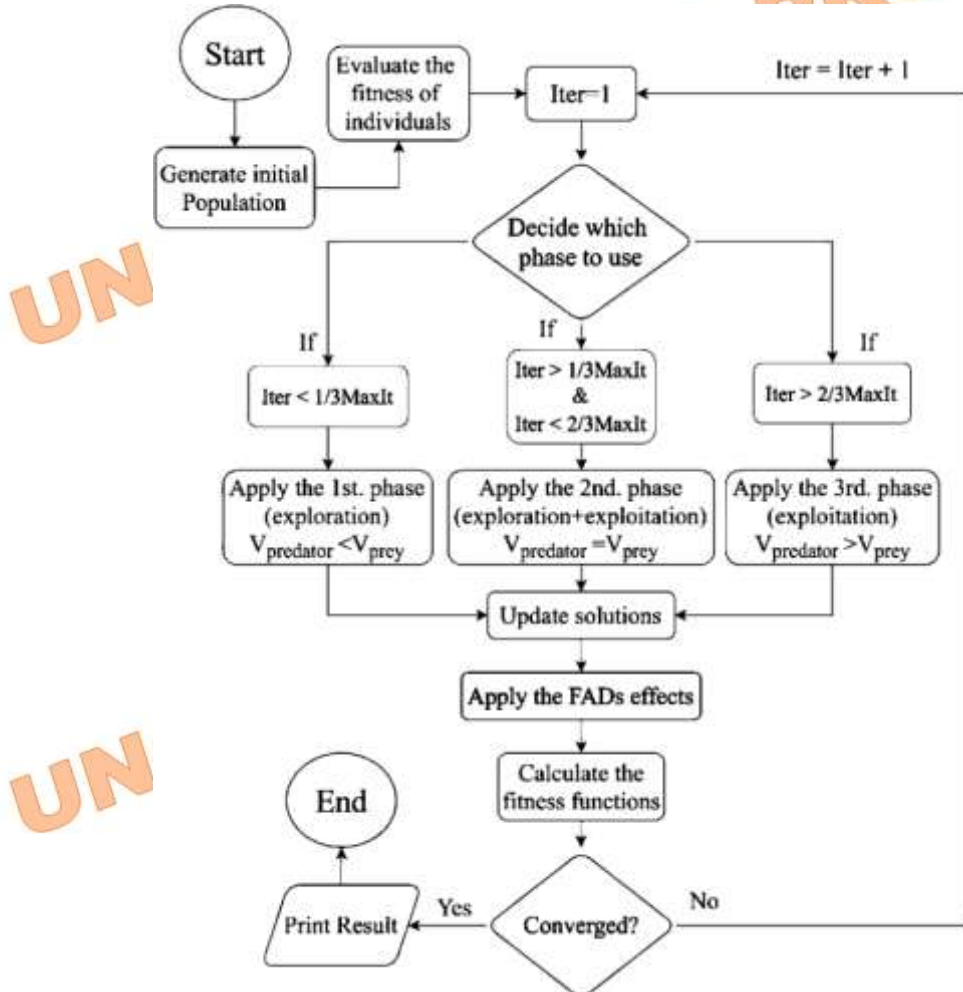


Fig. 6. The overall trend of the MPA

9. Kriging Interpolation Method

The foundation of this method was initially proposed by Danie G. Krige and quickly gained popularity as an efficient and cost-effective simulation technique. [105]. The Kriging estimation method focuses on interpolating data based on spatial variance, which depends on the distance between points. This model is also sufficiently flexible to capture nonlinear functions. Kriging is widely applied in reliability assessments and failure probability analyses [106, 107]. When considering the response function $G(x)$, the basic Kriging model is formulated as Equation 20. $G(x)$ is composed of two components: the first part, $F(x, \beta)$, represents regression models, while the second part, $Z(x)$, corresponds to random processes [108, 109]:

$$G(x) = F(x, \beta) + Z(x) + f(x)^T \beta + Z(x) \quad (20)$$

where: $[f_1(x), f_1(x), \dots, f_m(x)]^T$ and $\beta^T = [\beta_1, \beta_1, \dots, \beta_m]$ are the basis functions and the corresponding regression coefficient. $F(x, \beta) = F(x, \beta) + Z(x)$ is a Gaussian function with a mean value of zero Covariance is presented as follows:

$$\text{Cov}(p, r) = \sigma^2 R(\theta, p, r) \quad (21)$$

where σ^2 and $R(\theta, p, r)$ are selected respectively, as the variance and Gaussian correlation function between the points p and r using the parameter θ [109].

10. How to Set the Parameters of ML Methods

Machine learning methods contain several regulatory parameters; if they are set optimally,

they will improve the accuracy of the method. In the GMDH method, in each layer, a limited number of neurons (Neurons with less error) are selected to form the next generation. The criterion error for selecting neurons is determined from the following equation:

$$e_c = \alpha e_{\min} + (1 - \alpha) e_{\max} \quad (22)$$

where e_{\min} and e_{\max} are the minimum and maximum error in each layer, and α is the factor of selection pressure.

In the fuzzy network, the fuzzy clustering algorithm (FCM) is utilized, and its function is introduced in MATLAB software as "genfis3". The regulatory parameters of the fuzzy method include the following:

1. Number of clusters: This parameter determines the number of clusters the algorithm will attempt to identify in the data.
2. Type of input and output membership functions: Fuzzy logic systems use membership functions to represent the degree of membership of elements in a set. The type of these membership functions (e.g., Gaussian, triangular, etc.) can significantly influence the performance of the FCM.
3. Iterations number: This parameter specifies the maximum number of iterations allowed for the algorithm to converge and achieve a solution.

Details of the setting parameters can be found in Table 4.

Table 4. Details of the parameters of the methods used

ELM parameters						
N.Iteration	N. Hidden neurons	Activation function				
20	17	Hyperbolic tangent sigmoid ($f(x)=\frac{e^x-e^{-x}}{e^x+e^{-x}}$)				
GMDH parameters						
N.Iteration	α	N. Layer Neurons				
100	0.7	Minimum (75 and number of neurons that $e<e_c$ with $\alpha=0.7$)				
MPA parameters						
N.O. population		N.O.Iteration	FADs		Constant number	
50		100	0.2		0.5	
ANFIS parameters						
train_StepSizeIncrease	train_StepSizeDecrease	N.O.Epoch	N.O.Iteration	Membership Function Type		
				Output	Input	N.O.Cluster
1.15	0.95	250	150	linear	gussmf	20
Kriging						
Correlation Functions		Regression Polynomial		Threshold for equal		
Exponential		1 degree		1e-14		

11. Results and Discussion

The performance of the machine learning methods used in this study was compared to

previous study models to estimate the compressive strength of R/S columns confined by FRP. For this purpose, two models that were

selected as the best methods of previous studies by Moodi et al. [48] study are compared with the methods of this study. To evaluate the performance of methods of this study, widely-used indicators have been used in Moodi et al. [48] study are used in this study. These indicators include Standard Deviation (SD), Mean Squared Error (MSE), Absolute Integral Error (IAE), and total Error (e_{Total}).

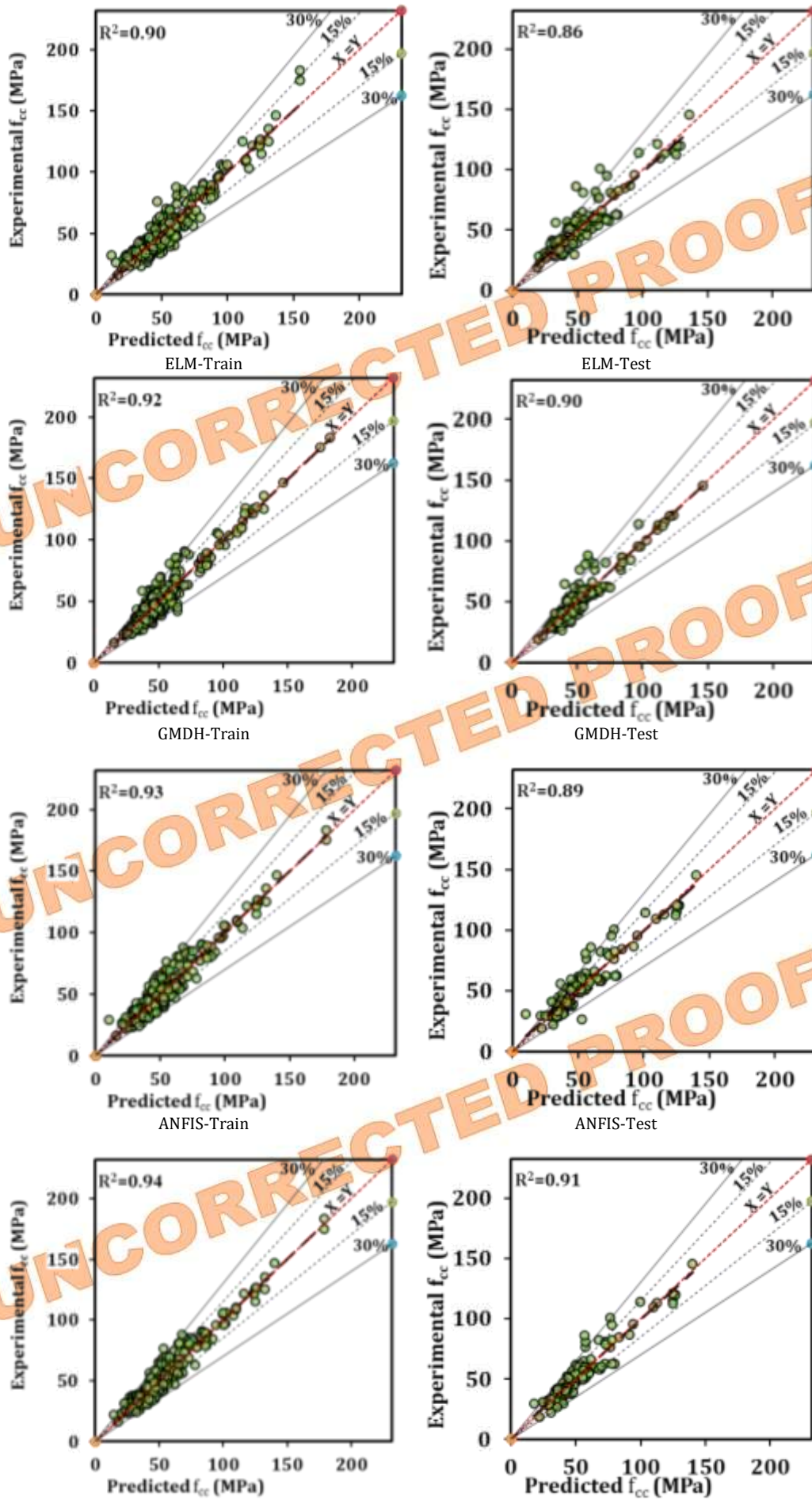
12. Comparison of Accuracy of the Proposed ML Methods

To compare the accuracy of ML methods, statistical indices were computed separately for training and test specimens, as shown in Table 5. The statistical indices of test specimens were used for comparison since these specimens were not involved in training. If the indices of the test specimens are equal, the indices of the training specimens can be considered. As shown in Table 5, statistical indices of the Kriging method are less than those of the other models, in both training and testing specimens. Also, the total error of the ANFIS-MPA and GMDH methods is almost equal for test specimens. Among other statistical indicators for the test specimens, the ANFIS-MPA method performed better than the GMDH method with a slight difference. Therefore, it is better to use training specimens to specify the method with better performance between the ANFIS-MPA and GMDH methods. The statistical

indicators of the training specimens for the ANFIS-MPA method are smaller than those of the GMDH method. Thus, the total error of the ANFIS-MPA method is approximately 9% less than the total error of the GMDH method. This difference can also be seen in the statistical indices of all specimens. Therefore, in this study, the Kriging method can be selected as the best method, and the ANFIS-MPA method as the next best method. It is noteworthy that when the difference between training statistical indicators and test ones is large, it indicates that this method does not work well. For this purpose, the average ratio of statistical indicators of training specimens to test ones was calculated, which is equal to 0.98, 0.99, 0.87, 0.93, and 0.08 for ELM, GMDH, ANFIS, ANFIS-MPA, and Kriging methods, respectively. This indicates that the difference between the statistical indices of the training and test specimens in the Kriging method is greater than in the others and that there is the least difference in the GMDH method. Thus, the GMDH method can be selected as one of the best methods for estimating the compressive strength of FRP-confined concrete. It is noteworthy that the large difference between the statistical indicators of training and test specimens in the Kriging method is due to its very small statistical indicators for training specimens. Otherwise, the statistical indicators of test specimens in this method are lower than those of other models.

Table 5. Statistical indicators related to LM methods

	Method	MSE	AAE	SD	e_{tot}
Train	ELM	2.53	12.54	15.96	11.50
	GMDH	1.80	9.83	13.36	9.27
	ANFIS	1.94	10.70	14.38	9.78
	ANFIS-MPA	1.47	9.22	12.57	8.52
	Kriging	0.019	0.45	1.40	0.55
Test	ELM	2.57	12.42	16.14	12.26
	GMDH	1.80	9.87	13.47	9.29
	ANFIS	2.66	11.08	16.37	10.45
	ANFIS-MPA	1.61	9.65	12.79	9.39
	Kriging	1.02	7.028	10.17	6.72
Total	ELM	2.54	12.51	16.00	11.73
	GMDH	1.80	9.84	13.38	9.28
	ANFIS	2.16	10.82	14.76	9.98
	ANFIS-MPA	1.51	9.35	12.34	8.78
	Kriging	0.321	2.42	5.68	2.36



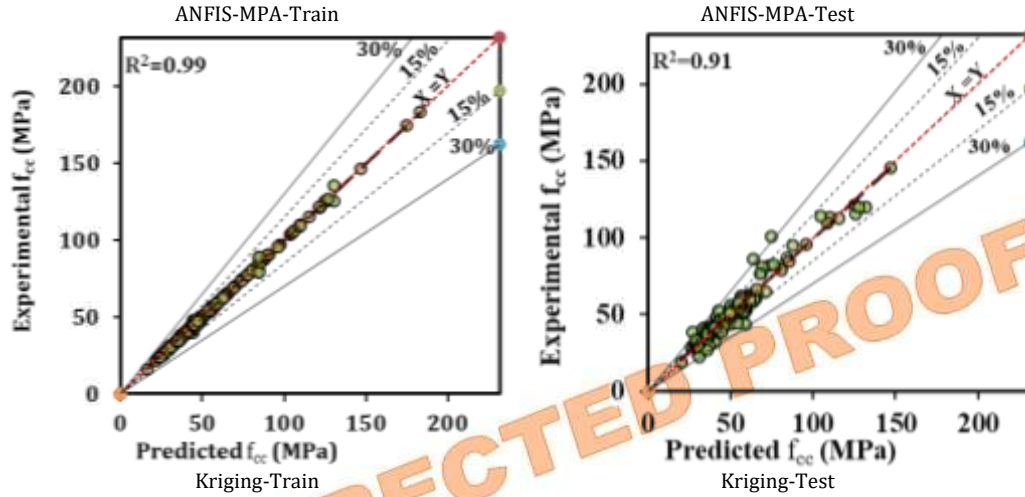


Fig. 7. Estimated and actual values of compressive strength through ML methods

To illustrate the efficiency of ML methods, Fig. 7 presents the experimental compressive strength versus the compressive strength predicted by ML models, separately for test and training specimens. To enhance the visualization and facilitate interpretation, additional reference lines at $\pm 15\%$ and $\pm 30\%$ error margins have been included in the plot. These lines help the reader assess the deviation of predicted values from experimental data. Points located within the 15% band indicate highly accurate predictions, whereas those within the 30% band still suggest reasonable estimations but with higher variability. As shown in Fig. 7, data points in the Kriging method are more closely distributed around the midline, indicating higher prediction accuracy. The Kriging method has the majority of its data points within the 15% margin, reinforcing its superior performance. The correlation coefficient (R^2) for the Kriging method is 0.95 for test specimens, which is the highest among all models. Following the Kriging method, the hybrid ANFIS-MPA model demonstrates better alignment with the midline, with an R^2 value of 0.91 for test specimens. This suggests that ANFIS-MPA also provides reliable predictions but with slightly lower accuracy compared to Kriging.

The results show that when the classic training algorithm of the Mamdani system was replaced by the MPA, in the ANFIS method, statistical indicators were reduced. For example, the total error of the ANFIS-MPA method is reduced by 13, 10, and 12% for the training, testing, and total specimens, respectively, compared to the ANFIS method with the Mamdani algorithm.

13. Comparison of ML Methods and the Models of Previous Studies

To compare the performance of the two best models of previous studies (Moodi et al. [13] and Wei and Wu [9]) with ML methods should be used with statistical indices of total specimens because models of previous studies have not been trained with the database. Those statistical indices are presented in Table 6.

According to Table 6, the two best methods of ML perform much better than the two best models of previous studies. On average, the error of the two best methods of ML is 62% less than the two best models of previous studies. Specifically, the total error (*etot*) of the Kriging method is 81.7% lower than that of Moodi et al. [13] and 85.7% lower than that of Wei and Wu [9]. Similarly, the ANFIS-MPA model reduces the total error by 32.0% compared to Moodi et al. [13] and by 46.8% compared to Wei and Wu [9]. It should be noted that among the ML methods, the ELM method has the highest error, so this method performs poorer than Moodi et al. [13] (Best models of previous studies).

To show the performance of ML and the models of past studies, experimental compressive strength against compressive strength computed from GMDH, ELM, ANFIS, ANFIS-MPA, and Kriging methods, and Moodi et al. [13] and Wei and Wu [9] Models are drawn in Fig. 8. Amongst ML methods and the models of past studies, ML methods are closer to the midline and have had a higher correlation coefficient (R^2), according to Table 6. Among the ML methods, the correlation coefficient of the Kriging and ANFIS-MPA methods has been the highest.

Contrary to statistical indices, the correlation coefficient (R^2) of the ELM method is higher than the models of past studies, and this shows that the worst ML method works better than the models of previous studies. It should be noted that the speed of the ELM method is very high.



Semnan University

Mechanics of Advanced Composite Structures

Journal homepage: <https://macs.semnan.ac.ir/>

ISSN: 2423-7043



Table 6. Statistical parameters for confined-FRP concrete specimens

Method	MSE	AAE	SD	e_{tot}	R^2
Moodi et al. [13]	2.43	12.15	15.59	12.91	0.87
Wei and Wu [9]	3.73	14.90	18.74	16.51	0.86
ELM	2.50	12.10	15.80	11.29	0.89
GMDH	1.80	9.84	13.38	9.28	0.92
ANFIS	2.16	10.82	14.76	9.98	0.92
ANFIS-MPA	1.51	9.35	12.34	8.78	0.93
Kriging	0.321	2.42	5.68	2.36	0.98

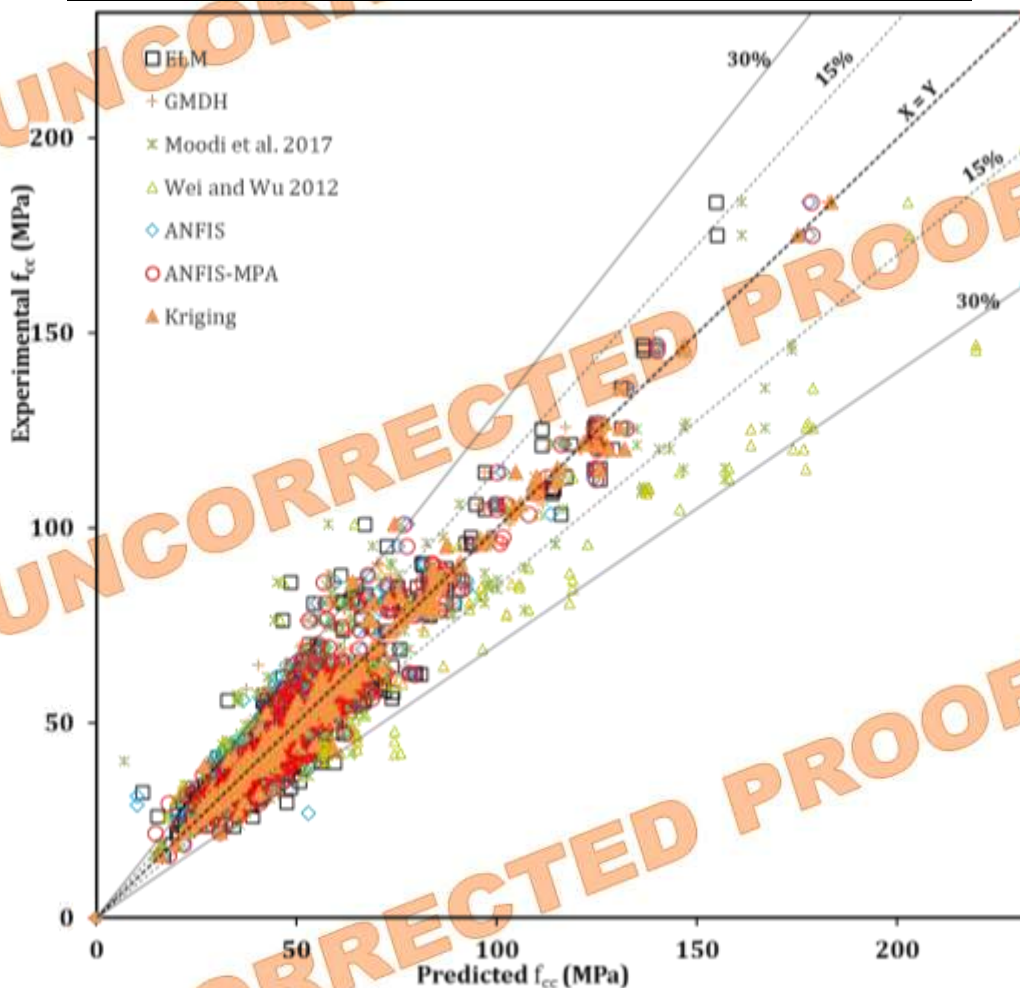


Fig. 8. Performance of total models

The results of this study and Moodi et al. [48] study show that the Kriging method has better performance than the MLP method in Moodi et al. [48] study so the correlation coefficient of the

Kriging method is 2% higher than the MLP method.

Fig. 9 shows box plots of the ratio of the compressive strength of confined-FRP concrete

* Corresponding author.

E-mail address: m.ghasemi@velayat.ac.ir

Cite this article as:

Mohammadi, A. and Mahdi-Nia, M., 2025. Title of article. *Mechanics of Advanced Composite Structures*, 12(1), pp. xx-xx

<https://doi.org/10.22075/MACS.2024.39315.2050>

predicted by different models to that found from experiments. In this plot, if the mean of the data is lying next to one, it means the models have had precise estimations of the compressive strength. The short length of the box plot in the models means greater certainty and a high level of agreement in their predicted results. The length of the box plot in Moodi et al. [13], Wei and Wu [9], and ELM models is higher than other methods, showing greatly dispersed and scattered data in them. According to the length of the box plot, the Kriging model had the highest certainty. The box plot length of the ANFIS-MPA

model is the second shortest box length, so the data scatter in the Kriging method is less than the ANFIS-MPA method. In all methods, the median of the data is greater than one, indicating that none of these methods is conservative and that the estimated value is slightly higher than the experimental value. But in the Kriging and ANFIS-MPA methods, the median of the data is very close to one, which indicates that the performance of these two methods is better than the other methods. In the ANFIS-MPA method, data scatter is high and this method cannot be selected as a suitable method.

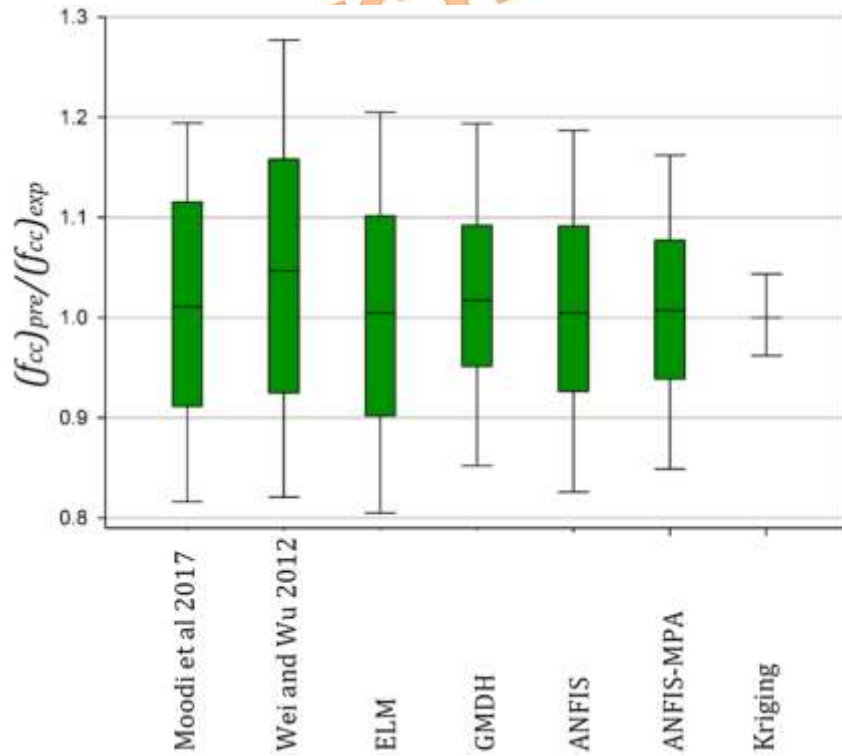


Fig. 9. Box plots of the “predicted-to-experimental” FRP-confined concrete strength ratios for different models, highlighting accuracy and dispersion

Fig. 10 illustrates the cumulative frequency plots obtained for seven models investigated in this study. This figure shows that the Kriging method had the higher portions of data points estimated at low absolute relative error and Wei and Wu [9] had the lowest of those. For example,

for an absolute relative error of 0.2, the cumulative frequency is around 59%, 43%, 56%, 59%, 63%, 70%, and 76% for Moodi et al. [13], Wei and Wu [9], ELM, GMDH, ANIS, ANFIS-MPA, and Kriging methods, respectively.



Semnan University

Mechanics of Advanced Composite Structures

Journal homepage: <https://macs.semnan.ac.ir/>

ISSN: 2423-7043

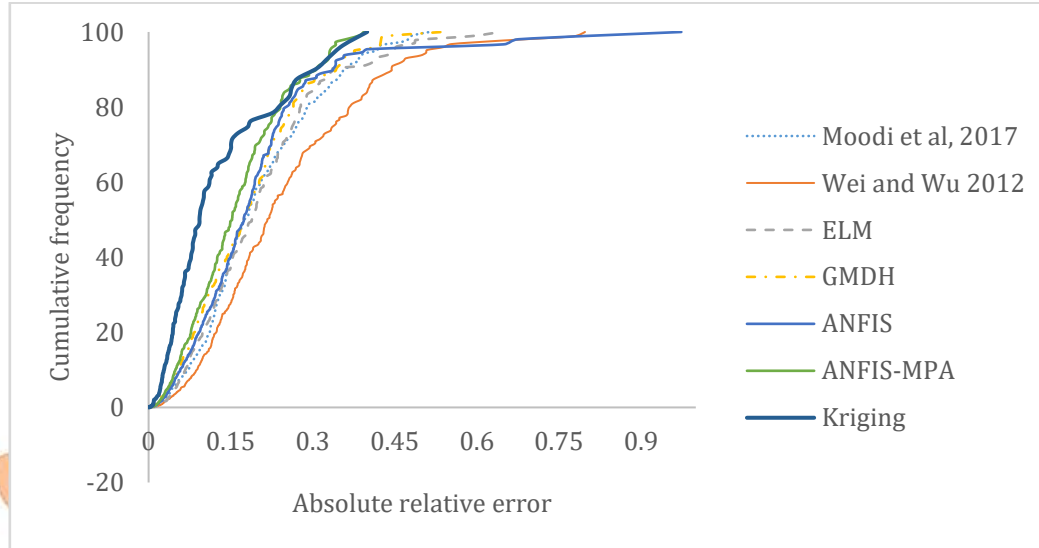


Fig. 10. Cumulative frequency versus the absolute average relative deviation

14. Sensitivity Analysis

In this section, the importance of each input parameter, including b , h , r , t_f , F_f/f_{co} , and E_f/f_{co} , on the output parameter (f_{cc}) is investigated. Equation 23 is employed to show the contribution of each parameter. The provided equation suggests that as the value of "S" increases for each parameter, the corresponding parameter has a greater impact on the model output. This implies that variations or changes in the input parameters, particularly those with higher "S" values, have a more pronounced effect on the overall output of the model.

$$S(X_i, Y) = \frac{\sum_{i=1}^n (X_i - \bar{X})(Y_i - \bar{Y})}{\sqrt{\sum_{i=1}^n (X_i - \bar{X})^2 \sum_{i=1}^n (Y_i - \bar{Y})^2}} \quad (23)$$

In the above equation, X_i and Y_i represent the input parameter and the output for the given input parameter X_i , respectively. \bar{X} and \bar{Y} denote the mean of the input parameters and the output values, respectively. n represents the number of data. The sensitivity analysis results, according to Equation 23, are presented in Table 7.

Table 7. Results of sensitivity analysis

	b	h	r	t_f	t_f/b	t_f/h	F_f/f_{co}	E_f/f_{co}
S	0.22	0.43	0.32	0.11	-0.14	-0.10	0.46	0.43

A positive or negative "S" value in the input variables indicates a direct or inverse effect of the input variable on the output variable, respectively. Among the eight investigated parameters, t_f/b and t_f/h parameters have an inverse effect on the output parameter. Also, E_f/f_{co} , F_f/f_{co} , and r/h parameters having the highest S value, have the highest effect on the compressive strength of confined concrete pressure resistance, and r/t_f , and t_f/h variables have the least effect on the output variable.

15. Conclusion

In this study, a database of FRP-confined concrete with rectangular/square (R/S) cross-sections has been collected and used to find the method for determining the compressive strength. For this purpose, several methods of machine learning (ML) methods were compared with each other. These methods included ELM, GMDH, ANFIS, ANFIS-MPA, and Kriging. The novelty of this study is finding a suitable method for estimating the compressive strength of those specimens with all types of concrete and FRP sheets. The database of this study consisted of 485 samples, 30% and 70% of which were used

* Corresponding author.

E-mail address: m.ghasemi@velayat.ac.ir

Cite this article as:

Mohammadi, A. and Mahdi-Nia, M., 2025. Title of article. *Mechanics of Advanced Composite Structures*, 12(1), pp. xx-xx

<https://doi.org/10.22075/MACS.2024.39315.2050>

for training and testing, respectively. By comparing the results of ML methods with each other and with the models of past studies, the following results are obtained:

- The obtained findings from this study show that the ML methods are more accurate than the previous study relationship for estimating the compressive strength of confined-FRP concrete with R/S cross-section.
- The use of ML methods reduces the error by an average of 43% compared to the two best relationships of previous studies. Also, the correlation coefficient (R^2) of the ML methods is 7% higher than that of past studies.
- Amongst the ML methods in this study, the Kriging and ANFIS-MPA methods have better accuracy than the other methods, with the correlation coefficient of Kriging and ANFIS-MPA being 0.98 and 0.93, respectively.
- In all comparisons of methods (statistical indicators, box plots, cumulative frequency), the Kriging method is better than the ANFIS-MPA method. Also, the Kriging method has better accuracy than the MLP method in Moodi et al. [48] study.
- Using the MPA instead of the Mamdani system in the ANFIS method reduces the total error by 12% for total specimens.

Conflicts of Interest

The authors declare that they have no conflict of interest.

Funding Statement

The research leading to these results received funding from [University Of Velayat] under Grant Agreement No [P-99-1-32].

References

- [1] Nanni, A. and Bradford, N.M., 1995. FRP jacketed concrete under uniaxial compression. *Construction and Building Materials*, 9, pp.115–124.
- [2] Saadatmanesh, H., Ehsani, M.R. and Li, M.W., 1994. Strength and Ductility of Concrete Columns Externally Reinforced With Fiber Composite Straps. *ACI Structural Journal*, 91, pp.434–447
- [3] Saafi, M., Toutanji, H. and Li, Z., 1999. Behavior of concrete columns confined with fiber reinforced polymer tubes. *ACI Materials Journal*, 96, pp.500–509
- [4] Mirmiran, A. and Shahawy, M., 1996. A new concrete-filled hollow FRP composite column. *Composites Part B: Engineering*, 27, pp.263–268.
- [5] Harajli, M.H., Hantouche, E.G. and Soudki, K., 2006. Stress-strain model for fiber-reinforced polymer jacketed concrete columns. *ACI Structural Journal*, 103, pp.672–682
- [6] Ilki, A. and Kumbasar, N., 2003. Compressive behaviour of carbon fibre composite jacketed concrete with circular and non-circular cross-sections. *Journal of Earthquake Engineering*, 7, pp.381–406.
- [7] Lam, L. and Teng, J.G., 2003. Design-Oriented Stress-Strain Model for FRP-Confined Concrete in Rectangular Columns. *Journal of Reinforced Plastics and Composites*, 22, pp.1149–1186.
- [8] Pham, T.M. and Hadi, M.N.S., 2014. Stress Prediction Model for FRP Confined Rectangular Concrete Columns with Rounded Corners. *Journal of Composites for Construction*, 18, pp.04013019.
- [9] Wei, Y.Y. and Wu, Y.F., 2012. Unified stress-strain model of concrete for FRP-confined columns. *Construction and Building Materials*, 26, pp.381–392.
- [10] Toutanji, H., Han, M., Gilbert, J. and Matthys, S., 2010. Behavior of Large-Scale Rectangular Columns Confined with FRP Composites. *Journal of Composites for Construction*, 14, pp.62–71.
- [11] Moodi, Y., Mousavi, S.R., Ghavidel, A., Sohrabi, M.R. and Rashki, M., 2018. Using Response Surface Methodology and providing a modified model using whale algorithm for estimating the compressive strength of columns confined with FRP sheets. *Construction and Building Materials*, 183, pp.163–170.
- [12] Moodi, Y., Mousavi, S.R. and Sohrabi, M.R., 2019. New models for estimating compressive strength of concrete confined with FRP sheets in circular sections. *Journal of Reinforced Plastics and Composites*, 38, pp.1014–1028.
- [13] Moodi, Y., Farahi Shahri, S. and Mousavi, S.R., 2017. Providing a model for estimating the compressive strength of square and rectangular columns confined with a variety of fibre-reinforced polymer sheets. *Journal of Reinforced Plastics and Composites*, 36, pp.1602–1612.
- [14] Naderpour, H. and Mirrashid, M., 2020. Confinement Coefficient Predictive Modeling of FRP-Confined RC Columns.

- Advances in Civil Engineering Materials*, 9, pp.20190145.
- [15] Kamgar, R., Naderpour, H., Komeleh, H.E., Jakubczyk-Gańczyńska, A. and Jankowski, R., 2020. A Proposed Soft Computing Model for Ultimate Strength Estimation of FRP-Confined Concrete Cylinders. *Applied Sciences*, 10, pp.1769.
- [16] Abbaszadeh, M.A. and Sharbatdar, M., 2020. Modeling of Confined Circular Concrete Columns Wrapped by Fiber Reinforced Polymer Using Artificial Neural Network. *Journal of Soft Computing in Civil Engineering*, 4, pp.61–78.
- [17] Teng, J.G., Chen, J.F., Smith, S.T. and Lam, L., 2015. Behaviour and strength of FRP-strengthened RC structures: a state-of-the-art review. *Proceedings of the Institution of Civil Engineers - Structures and Buildings*, 156, pp.51–62.
- [18] Mansouri Nejad, N., Beheshti Aval, S.B., Maldar, M. and Asgarian, B., 2020. A damage detection procedure using two major signal processing techniques with an artificial neural network on a scaled jacket offshore platform. *Advances in Structural Engineering*, 156, pp.1655–1667.
- [19] Dai, B., Gu, C., Zhao, E., Zhu, K., Cao, W. and Qin, X., 2018. Improved online sequential extreme learning machine for identifying crack behavior in concrete dam. *Advances in Structural Engineering*, 22, pp.402–412.
- [20] Su, L. and He, H.J., 2019. Decision tree-based seismic damage prediction for reinforcement concrete frame buildings considering structural micro-characteristics. *Advances in Structural Engineering*, 22, pp.2097–2109.
- [21] Pham, T.M. and Hao, H., 2016. Prediction of the impact force on reinforced concrete beams from a drop weight. *Advances in Structural Engineering*, 19, pp.1710–1722.
- [22] Shahri, S.F. and Mousavi, S.R., 2021. Bond strength prediction of spliced GFRP bars in concrete beams using soft computing methods. *Computers and Concrete*, 24, pp.305–317.
- [23] Mousavi, S.M., Bahr Peyma, A., Mousavi, S.R. and Moodi, Y., 2023. Predicting the Ultimate and Relative Bond Strength of Corroded Bars and Surrounding Concrete by Considering the Effect of Transverse Rebar Using Machine Learning. *Iranian Journal of Science and Technology, Transactions of Civil Engineering*, 47, pp.193–219.
- [24] Jamali, F., Mousavi, S.R., Peyma, A.B. and Moodi, Y., 2022. Prediction of compressive strength of fiber-reinforced polymers-confined cylindrical concrete using artificial intelligence methods. *Journal of Reinforced Plastics and Composites*, 41, pp.679–704.
- [25] Rezazadeh Eidgahee, D., Rafiean, A.H. and Haddad, A., 2020. A Novel Formulation for the Compressive Strength of IBP-Based Geopolymer Stabilized Clayey Soils Using ANN and GMDH-NN Approaches. *Iranian Journal of Science and Technology - Transactions of Civil Engineering*, 44, pp.219–229.
- [26] Parhi, S.K. and Panigrahi, S.K., 2024. Alkali-silica reaction expansion prediction in concrete using hybrid metaheuristic optimized machine learning algorithms. *Asian Journal of Civil Engineering*, 25, pp.1091–1113.
- [27] Kandavel, T.K., Kumar, T.A. and Varamban, E., 2020. Prediction of tribological characteristics of powder metallurgy Ti and W added low alloy steels using artificial neural network. *Indian Journal of Engineering and Materials Sciences (IJEMS)*, 27, pp.503–517.
- [28] Stephen, D.S. and Prabhu, S., 2022. Surface Roughness Prediction in Grinding Ti using ANFIS Hybrid Algorithm. *Indian Journal of Engineering and Materials Sciences*, 29, pp.666–675.
- [29] Ilkhani, M.H., Naderpour, H. and Kheyroddin, A., 2019. Soft computing-based approach for capacity prediction of FRP-strengthened RC joints. *Scientia Iranica*, 26, pp.2678–2688.
- [30] Rezaie-Balf, M., 2019. Multivariate Adaptive Regression Splines Model for Prediction of Local Scour Depth Downstream of an Apron Under 2D Horizontal Jets. *Iranian Journal of Science and Technology - Transactions of Civil Engineering*, 43, pp.103–115.
- [31] Saha, P., Sapkota, S.C., Das, S. and Kwatra, N., 2024. Prediction of fresh and hardened properties of self-compacting concrete using ensemble soft learning techniques. *Multiscale and Multidisciplinary Modeling, Experiments and Design*, 7, pp.4923–4945.
- [32] Ali, B.H.S.H., Faraj, R.H., Saeed, M.A.H., Ahmed, H.U. and Ahmed, F.W., 2024. Innovative machine learning approaches to predict the compressive strength of recycled plastic aggregate self-compacting concrete incorporating different waste ashes. *Multiscale and Multidisciplinary Modeling, Experiments and Design*, 7, pp.2585–2604.

- [33] Tafarroj, M.M. and Hatami, H., 2024. Application of machine learning and fuzzy logic to predict the effect of impact loading on the life of rectangular reinforced panels as offshore reinforced concrete structures. *International Journal of Coastal, Offshore And Environmental Engineering(ijcoe)*, Available Online.
- [34] Chen, W., Xu, J., Dong, M., Yu, Y., Elchalakani, M. and Zhang, F., 2021. Data-driven analysis on ultimate axial strain of FRP-confined concrete cylinders based on explicit and implicit algorithms. *Composite Structures*, 268, pp.113904.
- [35] Moodi, Y., Sohrabi, M.R. and Mousavi, S.R., 2021. Corrosion effect of the main rebar and stirrups on the bond strength of RC beams. *Structures*, 32, pp.1444–1454.
- [36] DeRousseau, M.A., Laftchiev, E., Kasprzyk, J.R., Rajagopalan, B. and Srubar, W.V., 2019. A comparison of machine learning methods for predicting the compressive strength of field-placed concrete. *Construction and Building Materials*, 228, pp.116661.
- [37] Naderpour, H., Rezazadeh Eidgahee, D., Fakharian, P., Rafiean, A.H. and Kalantari, S.M. 2020. A new proposed approach for moment capacity estimation of ferrocement members using Group Method of Data Handling. *Engineering Science and Technology, an International Journal*, 23, pp.382–391.
- [38] Kumar, R. and Hynes, N.R.J., 2020. Prediction and optimization of surface roughness in thermal drilling using integrated ANFIS and GA approach. *Engineering Science and Technology, an International Journal*, 23, pp.30–41.
- [39] Amirkhani, A., Kolahdoozi, M., Wang, C. and Kurgan, L.A. 2020. Prediction of DNA-Binding Residues in Local Segments of Protein Sequences with Fuzzy Cognitive Maps. *IEEE/ACM Transactions on Computational Biology and Bioinformatics*, 17, pp.1372–1382.
- [40] Cihan, M.T., 2019. Prediction of Concrete Compressive Strength and Slump by Machine Learning Methods. *Advances in Civil Engineering*, 1, pp.1–11.
- [41] Faramarzi, A., Heidarinejad, M., Mirjalili, S. and Gandomi, A.H., 2020. Marine Predators Algorithm: A nature-inspired metaheuristic. *Expert Systems with Applications*, 152, pp.113377.
- [42] Wu, Y., Jin, G., Ting, D. and Dong, M., 2010. Modeling Confinement Efficiency of FRP-Confined Concrete Column Using Radial Basis Function Neural Network. *2nd International Workshop on Intelligent Systems and Applications*, Wuhan, China.
- [43] Pham, T.M. and Hadi, M.N.S., 2014. Predicting Stress and Strain of FRP-Confined Square / Rectangular Columns Using Artificial Neural Networks. *Journal of Composites for Construction*, 18, pp. 04014019.
- [44] Doran, B., Yetilmezsoy, K. and Murtazaoglu, S., 2015. Application of fuzzy logic approach in predicting the lateral confinement coefficient for RC columns wrapped with CFRP. *Engineering Structures*, 88, pp.74–91.
- [45] Lim, J.C., Karakus, M. and Ozbakkaloglu, T., 2016. Evaluation of ultimate conditions of FRP-confined concrete columns using genetic programming. *Computers & Structures*, 162, pp.28–37.
- [46] Sharifi, Y., Lotfi, F. and Moghbeli, A., 2019. Archive of SID Compressive Strength Prediction Using the ANN Method for FRP Confined Rectangular Concrete Columns. *Journal of Rehabilitation in Civil Engineering*, 7, pp.134–153.
- [47] Mohana, M.H., 2019. Reinforced concrete confinement coefficient estimation using soft computing models. *Periodicals of Engineering and Natural Sciences*, 7, pp.1833–1844.
- [48] Moodi, Y., Ghasemi, M. and Mousavi, S.R., 2021. Estimating the compressive strength of rectangular fiber reinforced polymer-confined columns using multilayer perceptron, radial basis function, and support vector regression methods. *Journal of Reinforced Plastics and Composites*, 41, pp.130–146.
- [49] Al-Salloum, Y.A., 2007. Influence of edge sharpness on the strength of square concrete columns confined with FRP composite laminates. *Composites Part B: Engineering*, 38, pp.640–650.
- [50] Benzaid, R., Chikh, N.E. and Mesbah, H., 2008. Behaviour of square concrete column confined with GFRP composite WARP. *Journal of Civil Engineering and Management*, 14, pp.115–120.
- [51] Campione, G., 2006. Influence of FRP wrapping techniques on the compressive behavior of concrete prisms. *Cement and Concrete Composites*, 28, pp.497–505.
- [52] Campione, G., Miraglia, N. and Scibilia, N., 2001. Compressive behavior of R.C.

- members strengthened with carbon fiber reinforced plastic layers. *Advances in Earthquake Engineering*, 9, pp.397–406.
- [53] Carrazedo, R., 2002. Mechanisms of confinement and its implication in strengthening of concrete columns with FRP jacketing. University of Sao Paulo.
- [54] Chaallal, O., Shahawy, M. and Hassan, M., 2003. Performance of Axially Loaded Short Rectangular Columns Strengthened with Carbon Fiber-Reinforced Polymer Wrapping. *Journal of Composites for Construction*, 7, pp.200–208.
- [55] Demers, M. and Neale, K.W., 1994. Strengthening of concrete columns with unidirectional composite sheets. *Proceedings of Developments in Short and medium Span Bridge Engineering*. Montreal, Que.
- [56] Erdil, B., Akyuz, U. and Yaman, I.O., 2012. Mechanical behavior of CFRP confined low strength concretes subjected to simultaneous heating-cooling cycles and sustained loading. *Materials and Structures/Materiaux et Constructions*, 45, pp.223–233.
- [57] Harries, K.A. and Carey, S.A., 2003. Shape and “gap” effects on the behavior of variably confined concrete. *Cement and Concrete Research*, 33, pp.881–890.
- [58] Hosotani, M., Kawashima, K. and HOSHIKUMA, J., 1997. A model for confinement effect for concrete cylinders confined by carbon fiber sheets. *Workshop on Earthquake Engineering Frontiers of Transportation Facilities*. Buffalo, New York, pp.405–430
- [59] Ignatowski, P. and Kamińska, M.E., 2003. On the effect of confinement of slender reinforced concrete columns with CFRP composites. 10, pp. 204–208
- [60] Masia, M.J., Gale, T.N. and Shrive, N.G., 2004. Size effects in axially loaded square-section concrete prisms strengthened using carbon fibre reinforced polymer wrapping. *Canadian Journal of Civil Engineering*, 31, pp.1–13.
- [61] Mirmiran, A., Shahawy, M. and Samaan, M., El Echary, H., Mastrapa, J.C. and Pico, O., 1998. Effect of Column Parameters on FRP-Confined Concrete. *Journal of Composites for Construction*, 2, pp.175–185.
- [62] Modarelli, R., Micelli, F. and Manni, O., 2005. FRP-Confinement of Hollow Concrete Cylinders and Prisms. *Proceedings of the 7th International Symposium on Fiber Reinforced Polymer Reinforcement of Reinforced Concrete Structures*, pp.1029–1046
- [63] Parvin, A. and Wang, W., 2001. Behavior of FRP Jacketed Concrete Columns under Eccentric Loading. *Journal of Composites for Construction*, 5, pp.146–152.
- [64] Rochette, P. and Labossière, P., 2000. Axial Testing of Rectangular Column Models Confined with Composites. *Journal of Composites for Construction*, 4, pp.129–136.
- [65] Rousakis, T.C., Karabinis, A.I. and Kioussis, P.D. 2007. FRP-confined concrete members: Axial compression experiments and plasticity modelling. *Engineering Structures*, 29, pp.1343–1353.
- [66] Rousakis, T.C. and Karabinis, A.I., 2012. Adequately FRP confined reinforced concrete columns under axial compressive monotonic or cyclic loading. *Materials and Structures*, 45, pp.957–975.
- [67] Shehata, I.A.E.M., Carneiro, L.A.V. and Shehata, L.C.D., 2002. Strength of short concrete columns confined with CFRP sheets. *Materials and Structures*, 34, pp.50–58.
- [68] Suter, R., Pinzelli, R., and Cambridge, U., 2001. Confinement of concrete columns with FRP sheets. *Proceedings of the 5th Symposium on Fibre Reinforced Plastic Reinforcement for Concrete Structures*, Thomas Telford, London, pp.793–802
- [69] Tao, Z., Yu, Q. and Zhong, Y.-Z., 2008. Compressive behaviour of CFRP-confined rectangular concrete columns. *Magazine of Concrete Research*, 60, pp.735–745.
- [70] Wang, L.M. and Wu, Y.F., 2008. Effect of corner radius on the performance of CFRP-confined square concrete columns: Test. *Engineering Structures*, 30, pp.493–505.
- [71] Wang, Y. and Wu, H., 2010. Experimental Investigation on Square High-Strength Concrete Short Columns Confined with AFRP Sheets. *Journal of Composites for Construction*, 14, pp.346–351.
- [72] Wang, Y. and Wu, H., 2011. Size Effect of Concrete Short Columns Confined with Aramid FRP Jackets. *Journal of Composites for Construction*, 15, pp.535–544.
- [73] Wang, Z., Wang, D. and Smith, S., 2012. Size effect of square concrete columns confined with CFRP wraps. *Proceedings of the Third Asia-Pacific Conference on FRP in Structures*, Hokkaido University, Japan.

- [74] Wang, Z., Wang, D., Smith, S.T. and Lu, D., 2012. CFRP-Confined Square RC Columns. I: Experimental Investigation. *Journal of Composites for Construction*, 16 pp.150–160.
- [75] Wu, Y.F. and Wei, Y.Y., 2010. Effect of cross-sectional aspect ratio on the strength of CFRP-confined rectangular concrete columns. *Engineering Structures*, 32, pp.32–45.
- [76] Yan, Z., Pantelides, C.P. and Reaveley, L.D., 2006. Fiber-reinforced polymer jacketed and shape-modified compression members: I - Experimental behavior. *ACI Structural Journal*, 103, pp.885–893
- [77] Yeh, F.Y. and Chang, K.C., 2012. Size and shape effects on strength and ultimate strain in frp confined rectangular concrete columns. *Journal of Mechanics*, 28, pp.677–690.
- [78] Youssef, M.N., Feng, M.Q. and Mosallam, A.S., 2007. Stress-strain model for concrete confined by FRP composites. *Composites Part B: Engineering*, 38, pp.614–628.
- [79] Zhang, D.J., Wang, Y.F. and Ma, Y.S., 2010. Compressive behaviour of FRP-confined square concrete columns after creep. *Engineering Structures*, 32, pp.1957–1963.
- [80] Ozbakkaloglu, T. and Oehlers, D.J., 2008. Concrete-Filled Square and Rectangular FRP Tubes under Axial Compression. *Journal of Composites for Construction*, 12, pp.469–477.
- [81] Ozbakkaloglu, T., 2013. Behavior of square and rectangular ultra high-strength concrete-filled FRP tubes under axial compression. *Composites Part B: Engineering*, 54, pp.97–111.
- [82] Ozbakkaloglu, T., 2012. Compressive behavior of square and rectangular high-strength concrete-filled FRP tubes. *Proceedings of the 12th International Symposium on Structural Engineering*, American Society of Civil Engineers, pp.965–970
- [83] Louk Fanggi, B.A. and Ozbakkaloglu, T., 2015. Square FRP-HSC-steel composite columns: Behavior under axial compression. *Engineering Structures*, 92, pp.156–171.
- [84] Fallah Pour, A., Gholampour, A., Zheng, J. and Ozbakkaloglu, T., 2019. Behavior of FRP-confined high-strength concrete under eccentric compression: Tests on concrete-filled FRP tube columns. *Composite Structures*, 220, pp.261–272.
- [85] Demir, U., Sahinkaya, Y., Ispir, M. and Ilki, A., 2018. Assessment of Axial Behavior of Circular HPFRCC Members Externally Confined with FRP Sheets. *Polymers*, 10, pp.138.
- [86] Ozbakkaloglu, T., 2014. Ultra-high-strength concrete-filled frp tubes: Compression tests on square and rectangular columns. *Key Engineering Materials*, Trans Tech Publications Ltd, pp.239–244
- [87] Huang, G.B., Zhu, Q.Y. and Siew, C.K., 2006. Extreme learning machine: Theory and applications. *Neurocomputing*, 70, pp.489–501.
- [88] Ding, S., Jia, W., Su, C., Zhang, L. and Liu, L., 2011. Research of neural network algorithm based on factor analysis and cluster analysis. *Neural Computing and Applications*, 20, pp.297–302.
- [89] Yaseen, Z.M., Deo, R.C., Hilal, A., Abd, A.M., Bueno, L.C., Salcedo-Sanz, S. and Nehdi, M.L., 2018. Predicting compressive strength of lightweight foamed concrete using extreme learning machine model. *Advances in Engineering Software*, 115, pp.112–125.
- [90] Al-shamiri, A.K., Kim, J.H., Yuan, T. and Yoon, Y.S., 2019. Modeling the compressive strength of high-strength concrete: An extreme learning approach. *Construction and Building Materials*, 208, pp.204–219.
- [91] Ivakhnenko, A.G., 1968. The Group Method of Data Handling-A Rival of the Method of Stochastic Approximation. *Soviet Automatic Control*, 1, pp.43–55
- [92] Farlow, S.J. 1984. Self-organizing methods in modeling: {GMDH} type algorithms. *CRC Press*, 54, pp.1–368
- [93] Ivakhnenko, A.G., 1971. Polynomial Theory of Complex Systems. *IEEE Trans Syst Man Cybern*, 1, pp.364–378.
- [94] Khalkhali, A. and Safikhani, H., 2012. Pareto based multi-objective optimization of a cyclone vortex finder using CFD, GMDH type neural networks and genetic algorithms. *Engineering Optimization*, 44, pp.105–118.
- [95] Mokfi, T., Shahnazar, A., Bakhshayeshi, I., Derakhsh, A.M. and Tabrizi, O., 2018. Proposing of a new soft computing-based model to predict peak particle velocity induced by blasting. *Engineering with Computers*, 34, pp.881–888.
- [96] Zadeh, L.A., 1965. Fuzzy Sets. *Information and Control*, 8, pp.338–353.
- [97] Saha, S.S., 2012. Basic principles of control systems in textile manufacturing. *Process*

- Control in Textile Manufacturing*, Woodhead Publishing Series in Textiles, pp.14-40.
- [98] Mehrdadi, N. and Ghasemi, M., 2021. Modeling of Tehran South Water Treatment Plant Using Neural Network and Fuzzy Logic Considering Effluent and Sludge Parameters. *Journal of Numerical Methods in Civil Engineering*, 6, pp.63-76
- [99] Köksal, F., Şahin, Y., Beycioğlu, A., Gencel, O. and Brostow, W., 2012. Estimation of fracture energy of high-strength steel fibre-reinforced concrete using rule-based Mamdani-type fuzzy inference system. *Science and Engineering of Composite Materials*, 19, pp.373-380.
- [100] Jang, J.S.R., Sun, C.T. and Mizutani, E., 2005. Neuro-Fuzzy and Soft Computing-A Computational Approach to Learning and Machine Intelligence. *IEEE Transactions on Automatic Control*, 42, pp.1482-1484.
- [101] Robati, F.N. and Iranmanesh, S., 2020. Inflation rate modeling: Adaptive neuro-fuzzy inference system approach and particle swarm optimization algorithm (ANFIS-PSO). *MethodsX*, 7, pp.101062.
- [102] Jang, J.S.R., 1993. ANFIS: Adaptive-Network-Based Fuzzy Inference System. *IEEE Transactions on Systems, Man, and Cybernetics: Systems*, 23, pp.665-685.
- [103] Abdel-Aleem, A., El-Sharief, M.A., Hassan, M.A. and El-Sebaie, M.G., 2017. Implementation of Fuzzy and Adaptive Neuro-Fuzzy Inference Systems in Optimization of Production Inventory Problem. *Applied Mathematics & Information Sciences*, 11, pp.289-298
- [104] Shaheen, M.A.M., Yousri, D., Fathy, A., Hasanien, H.M., Alkuhayli, A. and Muyeen, S.M., 2020. A Novel Application of Improved Marine Predators Algorithm and Particle Swarm Optimization for Solving the ORPD Problem. *Energies*, 13, pp.5679.
- [105] Jones, D.R., Schonlau, M. and Welch, W.J., 1998. Efficient Global Optimization of Expensive Black-Box Functions. *Journal of Global Optimization*, 13, pp.455-492.
- [106] Sacks, J., Welch, W.J., Mitchell, T.J. and Wynn, H.P., 1989. Design and Analysis of Computer Experiments. *Statistical Science*, 4, pp.409-423.
- [107] Zhou, Y., Lu, Z., Cheng, K. and Yun, W., 2019. A Bayesian Monte Carlo-based method for efficient computation of global sensitivity indices. *Mechanical Systems and Signal Processing*, 117, pp.498-516.
- [108] Matheron, G., 1973. The intrinsic random functions and their applications. *Advances in Applied Probability*, 5, pp.439-468.
- [109] Flores, E.I.S., DiazDelaO, F.A., Friswell, M.I. and Sienz, J., 2012. A computational multi-scale approach for the stochastic mechanical response of foam filled honeycomb cores. *Composite Structures*, 94, pp.1861-1870.